Molecular Biology of the Cell
Vol. 18, 4304–4316, November 2007

Saccharomyces cerevisiae CWH43 Is Involved in the Remodeling of the Lipid Moiety of GPI Anchors to Ceramides[D]

Mariko Umemura,*† Morihisa Fujita,* Takehiko Yoko-o,* Akiyoshi Fukamizu,‡ and Yoshifumi Jigami*†

*Research Institute for Cell Engineering, National Institute of Advanced Industrial Science and Technology, Ibaraki 305-8566, Japan; †Graduate School of Life and Environmental Science, University of Tsukuba, Ibaraki 305-8572, Japan; and ‡Center for Tsukuba Advanced Research Alliance, Graduate School of Life and Environmental Science, University of Tsukuba, Ibaraki 305-8577, Japan

Submitted May 22, 2007; Revised August 9, 2007; Accepted August 17, 2007
Monitoring Editor: Sean Munro

The glycosylphosphatidylinositol (GPI)-anchored proteins are subjected to lipid remodeling during their biosynthesis. In the yeast *Saccharomyces cerevisiae*, the mature GPI-anchored proteins contain mainly ceramide or diacylglycerol with a saturated long-fatty acid, whereas conventional phosphatidylinositol (PI) used for GPI biosynthesis contains an unsaturated fatty acid. Here, we report that *S. cerevisiae* Cwh43p, whose N-terminal region contains a sequence homologous to mammalian PGAP2, is involved in the remodeling of the lipid moiety of GPI anchors to ceramides. In *cwh43* disruptant cells, the PI moiety of the GPI-anchored protein contains a saturated long fatty acid and lyso-PI but not inositolphosphorylceramides, which are the main lipid moieties of GPI-anchored proteins from wild-type cells. Moreover, the C-terminal region of Cwh43p (Cwh43-C), which is not present in PGAP2, is essential for the ability to remodel GPI lipids to ceramides. The N-terminal region of Cwh43p (Cwh43-N) is associated with Cwh43-C, and it enhanced the lipid remodeling to ceramides by Cwh43-C. Our results also indicate that mouse FRAG1 and C130090K23, which are homologous to Cwh43-N and -C, respectively, share these activities.

INTRODUCTION

Many proteins are attached to the cell surface through glycosylphosphatidylinositol (GPI). GPI modification is conserved among mammalian cells, yeast, and protozoa (Ferguson, 1999; Kinoshita and Inoue, 2000; Pittet and Conzelmann, 2007). In the budding yeast *Saccharomyces cerevisiae*, ~60 proteins have been predicted to be GPI-anchored (Caro *et al*., 1997). Some of these proteins, such as Gas1p, seem to remain anchored to the plasma membrane, whereas the others become mainly cell wall-linked (Caro *et al*., 1997; Hamada *et al*., 1999; Kapteyn *et al*., 1999). Thus, yeast GPI-anchored proteins are mainly involved in cell wall integrity.

This article was published online ahead of print in *MBC in Press* (http://www.molbiolcell.org/cgi/doi/10.1091/mbc.E07–05–0482) on August 29, 2007.

[D] The online version of this article contains supplemental material at *MBC Online* (http://www.molbiolcell.org).

Address correspondence to: Yoshifumi Jigami (jigami.yoshi@aist.go.jp).

Abbreviations used: CFW, calcofluor white; Con A, concanavalin A; DRM, detergent-resistant membrane; DHS, dihydrosphingosine; ER, endoplasmic reticulum; IPC, inositolphosphorylceramide; IPC/B, IPC consisting of phytosphingosine and a C26:0 fatty acid; IPC/C, IPC consisting of phytosphingosine and a hydroxylated C26:0 fatty acid; mRFP, monomeric red fluorescent protein; PAGE, polyacrylamide gel electrophoresis; pG1, phosphatidylinositol with a C26:0 fatty acid in *sn*-2 position; PI, phosphatidylinositol; TLC, thin layer chromatography.

The biosynthesis of GPI and its attachment to the target protein are carried out on the endoplasmic reticulum (ER) membrane. GPIs, which have conserved core structures, are preassembled in the ER in a multistep pathway before their transfer to target proteins. GPIs are assembled by the sequential addition to PI of glucosamine, an acyl chain, mannoses, and ethanolamine phosphates. The complete GPIs are then attached to ER-translocated proproteins bearing a C-terminal signal sequence for GPI attachment. More than 20 genes involved in GPI biosynthesis and attachment to proteins have been identified, and, in most cases, these genes are conserved in yeast and mammalian cells (Kinoshita and Inoue, 2000; Orlean and Menon, 2007; Pittet and Conzelmann, 2007).

After the transfer of GPI to a protein, the acyl chain is removed from the inositol portion of GPI-anchored proteins (Tanaka *et al*., 2004; Fujita *et al*., 2006b). The inositol-deacylated GPI-anchored proteins are then transported to the plasma membrane by vesicular trafficking (Mayor and Riezman, 2004). GPI-anchored proteins are concentrated at the microdomains of plasma membrane, generally called lipid rafts, that are enriched with sterols and sphingolipids, and they can be isolated biochemically as detergent-resistant membrane (DRM) fractions (Simons and Ikonen, 1997). The lipid rafts are thought to play an important role in signal transduction and membrane trafficking.

Some mature GPI-anchored proteins have saturated fatty acid chains in the lipid moiety (McConville *et al*., 1993; Brewis *et al*., 1995; Benting *et al*., 1999), whereas GPI is synthesized from conventional PI, which usually has an unsaturated fatty acid chain. This conversion of the lipid

moiety is called "lipid remodeling" of GPI. In mammalian cells, after exchanging an unsaturated chain at the *sn*-2 position of the lipid moieties with a saturated chain, the lipid moieties of mature GPI-anchored proteins contain PI with two saturated fatty chains (Maeda *et al*., 2007). In contrast, mature GPI-anchored proteins in yeast contain two different types of lipid moieties (Conzelmann *et al*., 1992; Fankhauser *et al*., 1993; Sipos *et al*., 1994, 1997; Reggiori *et al*., 1997). One is diacylglycerol with a C26 fatty acid at the *sn*-2 position. The other type of lipid moiety is ceramide consisting mainly of C18:0 phytosphingosine (PHS) and C26:0 fatty acid (Sipos *et al*., 1997). In both types of lipid moieties, the C26 fatty acid may be hydroxylated (Sipos *et al*., 1997). However, which GPI-anchored proteins contain a ceramide-type lipid moiety in the GPI anchor remains unclear, although the ceramide type represents a major fraction of the total cells and Gas1p, a major GPI-anchored protein, is an example of protein containing diacylglycerol type of lipid moiety (Fankhauser *et al*., 1993).

The remodeling of the yeast lipid starts in the ER with the removal of the unsaturated acyl chain at the *sn*-2 position of diacylglycerol to form lyso-GPI. This GPI-phospholipase A_2 (GPI-PLA_2) activity requires Per1p (Fujita *et al*., 2006a). Next, a C26 saturated acyl chain is transferred to the *sn*-2 position by the *O*-acyltransferase Gup1p, generating diacylglycerol with a C26 fatty acid (Bosson *et al*., 2006). Recent studies suggest that these lipid remodeling events are required for both the efficient transport of GPI-anchored proteins from the ER to the Golgi and their association with lipid rafts (Bosson *et al*., 2006; Fujita *et al*., 2006a; Maeda *et al*., 2007). The diacylglycerol of the lipid moiety is replaced by ceramide consisting of PHS with a C26 fatty acid, a process that seems to occur in the ER (Sipos *et al*., 1997). In the Golgi, the ceramide of the lipid moiety is further changed to ceramide consisting of PHS with a hydroxy-C26 fatty acid (Reggiori *et al*., 1997; Sipos *et al*., 1997). The pathway for replacement by ceramide has not been elucidated, and proteins involved in this event have not been identified. Gpi7p and Mcd4p, which transfer ethanolamine phosphate to mannose during GPI biosynthesis, are reported to be indirectly involved in the remodeling of diacylglycerol to ceramides (Benachour *et al*., 1999; Zhu *et al*., 2006), but it remains unclear what proteins are directly responsible for this.

In this study, we found that yeast *CWH43* is required for the remodeling of the lipid moiety of GPI anchors to ceramides and that its C-terminal domain is especially important for this function. The N-terminal region of Cwh43p associated with C-terminal region is able to enhance the lipid remodeling to ceramides by C-terminal region. Furthermore, in yeast *cwh43*-disuruptant cells, the mouse *FRAG1* and *C130090K23* gene product, which are homologues of the N- and C-terminal regions of Cwh43p, respectively, can share these activities, indicating that the GPI lipid is remodeled to ceramides by mouse C130090K23 protein, whose function is enhanced when FRAG1 protein is introduced.

MATERIALS AND METHODS

Media and Strains

YPAD and synthetic complete (SC) media were described previously (Sherman, 1991). For [^{3}H]dihydrosphingosine (DHS) labeling, cells were cultured at 30°C in SC medium. The yeast strains used in this study included the following: *cwh43*Δ (*MAT***a** *his3Δ1 leu2Δ0 met15Δ0 ura3Δ0 cwh43Δ::KanMX4*; EUROSCARF), BY4741 (*MAT***a** *his3Δ1 leu2Δ0 met15Δ0 ura3Δ0*; wild-type strain), and *gpi7*Δ (*MAT***a** *his3Δ1 leu2Δ0 met15Δ0 ura3Δ0 gpi7Δ::KanMX4*; EUROSCARF).

Plasmids

Plasmids used in this report are listed in Table 1.

Construction of CWH43, CWH43-HA, and CWH43-mRFP Plasmids

The promoter region and open reading frame of *CWH43* were amplified by PCR (polymerase chain reaction) from genomic DNA by using primers CWH43-BamHI-F (5′-AAAAGGATCCGCAAACAATCTTGAAGGCT-3′) and CWH43-SalI-stop-NheI-R (5′-AAAAGTCGACTTAGCTAGCTAAGTAATA-ACGTGGCTCATCA-3′). The amplified fragment was digested with BamHI and SalI. The purified fragment was inserted into pRS316T, which contains the *GPI7* terminator region inserted into XhoI/KpnI-digested pRS316 (Sikorski and Hieter, 1989; Fujita *et al*., 2004, 2006a) to generate pRS316T-CWH43. A sequence encoding three copies of the hemagglutinin (HA) epitope was amplified and inserted into the NheI site of pRS316T-CWH43 to generate pRS316T-CWH43-HA. The DNA fragment encoding monomeric red fluorescent protein (mRFP; kindly provided by Dr. Roger Tsien, University of California, San Diego, La Jolla, CA) was also amplified and inserted into the NheI site of pRS316T-CWH43 to generate pRS316T-CWH43-mRFP.

Construction of Plasmid for Overexpression of CWH43-HA

The open reading frame of *CWH43* with a sequence encoding three copies of the HA epitope at the C terminus of the protein was amplified from pRS316T-CWH43-HA by using primers Kpn-CWH43-F18 (5′-GGGGTACCATGCT-GATCATCAATGGGAAG-3′) and HANheStpXba-R17 (5′-GCTCTAGATT-AGCTAGCGTAATCCGGTAC-3′). The amplified fragment was digested with KpnI and XbaI. The fragment was inserted into KpnI/XbaI-digested YEp352GAPII (Abe *et al*., 2003) to generate YEp352GAPII-CWH43-HA.

Construction of CWH43-N and CWH43-N-HA Plasmids

The short promoter region and the open reading frame encoding the N-terminal region (229 amino acids) of Cwh43p (CWH43-N) were amplified from pRS316T-CWH43 by using primers Xho-CWH43-P-N-F14 (5′-GATT-TCTCGAGGAATAAGTAAC-3′) and CWH43-N-NheStpXho-R15 (5′-CCG-CTCGAGGTCGACTTAGCTAGCACTAGAGTCTCTAATTTGGAAAA-3′). The amplified fragment was digested with XhoI. The fragment was inserted into pRS316T-CWH43, which contains the entire *CWH43* upper promoter region to generate pRS316T-CWH43-N. Three copies of the HA epitope were amplified and inserted into the NheI site of pRS316T-CWH43-N to generate pRS316T-CWH43-N-HA. The open reading frame of *CWH43-N* and the sequence encoding three copies of the HA epitope (*CWH43-N-HA*) were amplified from pRS316T-CWH43-N-HA by using primers Kpn-CWH43-F18 (5′-GGGGTACCATGCTGATCATCAATGGGAAG-3′) and HANheStpXba-R17 (5′-GCTCTAGATTAGCTAGCGTAATCCGGTAC-3′). The amplified fragment was digested with KpnI/XbaI. The fragment was inserted into KpnI/XbaI-digested YEp352GAPII to generate YEp352GAPII-CWH43-N-3HA.

Construction of CWH43-C and CWH43-C-HA Plasmids

The short promoter region and open reading frame encoding the C-terminal region (736 amino acids) of Cwh43p (CWH43-C) were amplified from pRS316T-CWH43 by using primers Xho-CWH43-P-C1-F11 (5′-TTTCTCGA-GGAATAAGTAACCAGGAATACAGAAGGTATCCACCGCCAGTTATGG-GTAATACCAGTTTTTTCCAAATT-3′) and NheStpXho-R12 (5′-CCGCT-CGAGGTCGACTTAGCTAG-3′). The amplified fragment was digested with XhoI. The fragment was inserted into pRS316T-CWH43, which contains the entire *CWH43* promoter region to generate pRS316T-CWH43-C. A sequence encoding three copies of the HA epitope were amplified and inserted into the NheI site of pRS316T-CWH43-C to generate pRS316T-CWH43-C-HA. The sequence encoding the open reading frame of *CWH43-C* and three copies of the HA epitope (CWH43-C-HA) were amplified from pRS316T-CWH43-C-HA by using primers Kpn-CWH43-C1-F19 (5′-GGGGTACCATGGGTAAT-ACCAGTTTTTTCCAA-3′) and HANheStpXba-R17 (5′-GCTCTAGATTAGC-TAGCGTAATCCGGTAC-3′). The amplified fragment was digested with KpnI/XbaI. The fragment was inserted into KpnI/XbaI-digested YEp352GAPII to generate YEp352GAPII-CWH43-C-HA.

Construction of Mutated cwh43-HA and cwh43-C-HA Plasmids

We substituted G57 with arginine by using the QuikChange site-directed mutagenesis kit (Stratagene, La Jolla, CA) and pRS316T-CWH43-HA, generating the plasmid pRS316T-CWH43-G57R-HA. We also substituted H472, D693, H770/H771, E807, D862, and R882 with alanine by using pRS316T-CWH43-C-HA, generating plasmids pRS316T-CWH43-C-H472A-HA, pRS316T-CWH43-C-D693A-HA, pRS316T-CWH43-C-H770AH771A-HA, pRS316T-CWH43-C-E807A-HA, pRS316T-CWH43-C-D862A-HA, and pRS316T-CWH43-C-R882A-HA, respectively.

Construction of FRAG1, FRAG1-HA, and FRAG1-FLAG Plasmids

The open reading frame of the mouse *FRAG1* gene was amplified from the plasmid of the National Institutes of Health mammalian gene collection clone (no. 3588752) by using primers EI-mmFRAG1-F24 (5′-GGAATTCATGTAC-

Table 1. Plasmids used in this study

Plasmid	Description	Origin
pRS315	*CEN, LEU2*	Sikorski and Hieter (1989)
pRS316	*CEN*, *URA3*	Sikorski and Hieter (1989)
YEp351GAPII	2 μ, *LEU2*, *TDH3* promoter and terminator	Abe *et al.* (2003)
YEp352GAPII	2 μ, *URA3*, *TDH3* promoter and terminator	Abe *et al.* (2003)
pRS316T	*GPI7* terminator, *pRS316*	Fujita *et al.* (2004)
pRS315T	*GPI7* terminator, *pRS315*	This study
pRS316T-CWH43	*CWH43*, *pRS316T*	This study
pRS316T-CWH43-HA	*CWH43-HA*, pRS316T	This study
pRS316T-CWH43-mRFP	*CWH43-mRFP*, pRS316T	This study
pRS316T-CWH43-GFP	*CWH43-GFP*, pRS316T	This study
pMF923	*mRFP-GAS1*, pRS315	Fujita *et al.* (2006a)
YEp352GAPII-CWH43-HA	*CWH43-HA*, YEp352GAPII	This study
pRS315T-CWH43-N-HA	*CWH43-N-HA*, pRS315T	This study
pRS316T-CWH43-N-HA	*CWH43-N-HA*, pRS316T	This study
pRS315T-CWH43-N-FLAG	*CWH43-N-FLAG*, pRS315T	This study
YEp352GAPII-CWH43-N-HA	*CWH43-N-HA*, YEp352GAPII	This study
YEp351GAPII-CWH43-N-HA	*CWH43-N-HA*, YEp351GAPII	This study
pRS316T-CWH43-C-HA	*CWH43-C-HA*, pRS316T	This study
YEp352GAPII-CWH43-C-HA	*CWH43-C-HA*, YEp352GAPII	This study
pRS316T-CWH43-G57R-HA	*cwh43-G57R-HA*, pRS316T	This study
pRS316T-CWH43-C-H472A-HA	*cwh43-C-H472A-HA*, pRS316T	This study
pRS316T-CWH43-C-D693A-HA	*cwh43-C-D693A-HA*, pRS316T	This study
pRS316T-CWH43-C-H770AH771A-HA	*cwh43-C-H770AH771A-HA*, pRS316T	This study
pRS316T-CWH43-C-E807A-HA	*cwh43-C-E807A-HA*, pRS316T	This study
pRS316T-CWH43-C-D862A-HA	*cwh43-C-D862A-HA*, pRS316T	This study
pRS316T-CWH43-C-R882A-HA	*cwh43-C-R882A-HA*, pRS316T	This study
YEp351GAPII-FRAG1-HA	*FRAG1-HA*, YEp351GAPII	This study
YEp352GAPII-FRAG1-HA	*FRAG1-HA*, YEp352GAPII	This study
YEp351GAPII-FRAG1-FLAG	*FRAG1-FLAG*, YEp351GAPII	This study
YEp352GAPII-C130090K23-HA	*C130090K23-HA*, YEp352GAPII	This study
YEp351GAPII-C130090K23-FLAG	*C130090K23-FLAG*, YEp351GAPII	This study
YEp352GAPII-C130090K23-FLAG	*C130090K23-FLAG*, YEp352GAPII	This study
YEp351GAPII-ALG13-FLAG	*ALG13-FLAG*, YEp351GAPII	This study
YEp352GAPII-ALG14-HA	*ALG14-HA*, YEp352GAPII	This study

CAGGTCCCACTGAC-3′) and mmFRAG1-NotI-R33 (5′-ATAAGAATGCG-GCCGCGAATCTCTTTTCCTCAGGCTG-3′). The amplified fragment was digested with EcoRI and NotI. The fragment was inserted into EcoRI/NotI-digested YEp352GAPII-HA, which contains three copies of the HA epitope, to generate YEp352GAPII-FRAG1-HA. A sequence encoding three copies of the FLAG epitope was amplified and inserted into the NotI/SalI site of YEp351GAPII-FRAG1-HA to generate YEp351GAPII-FRAG1-FLAG.

Construction of C130090K23, C130090K23-HA, and C130090K23-FLAG Plasmids

The open reading frame of the mouse *C130090K23* gene was amplified from the plasmid of the National Institutes of Health mammalian gene collection clone (no. 3584006) by using primers Sma-mmFLJ21511-F30 (5′-TCCCCCGG-GATGCCAGGCCTGTGGAGAG-3′) and mmFLJ21511-N*Sa-R27 (5′-TGCG-GTCGACTCAGCTAGCAACGAAGTATTTGGGTGTATTCA-3′). The amplified fragment was digested with SmaI and SalI. The fragment was ligated into SmaI/SalI-digested YEp352GAPII to generate YEp352GAPII-C130090K23. A sequence encoding three copies of the HA or FLAG epitopes were amplified and inserted into the NheI site of YEp352GAPII-C130090K23 to generate YEp352GAPII-C130090K23-HA or YEp352GAPII-C130090K23-FLAG.

Construction of ALG13-FLAG and ALG14-HA Plasmids

The open reading frame of *ALG13* was amplified by polymerase chain reaction (PCR) from genomic DNA by using primers Sac-ALG13-F (5′-CGAGCT-CATGGGTATTATTGAAGAAAAGGC-3′) and ALG13-Not-R (5′-ATAGTT-TAGCGGCCGCGCTGTATATAGTTTCAACTAGCA-3′). The amplified fragment was digested with SacI and NotI. The fragment was inserted into SacI/NotI-digested YEp351GAPII-FRAG1-FLAG, which contains three copies of the FLAG epitope, to generate YEp351GAPII-ALG13-FLAG. The open reading frame of *ALG14* was amplified by PCR from genomic DNA by using primers Sac-ALG14-F (5′-CGAGCTCATGAAAACGGCCTACTTGGC-3′) and ALG14-Not-R (5′-ATAGTTTAGCGGCCGCAACAAGGATGCCGAACCACTT-3′). The amplified fragment was digested with SacI and NotI. The fragment was inserted into SacI/NotI-digested YEp352GAPII-FRAG1-HA, which contains three copies of the HA epitope, to generate YEp352GAPII-ALG14-HA.

Fluorescence Microscopy

For imaging of Cwh43p-mRFP fusion protein, cells were grown to the exponential phase at 30°C in SC−uracil medium and washed twice. The cellular localization of Cwh43p-mRFP was visualized by fluorescence microscopy by using an Olympus IX-71 fluorescence microscope system (Olympus, Tokyo, Japan) and processed using IPLab software (Scanalytics, Fairfax, VA).

Analysis of PI Moieties of GPI-anchored Protein

Isolation of the radiolabeled lipid moieties of GPI anchor and lipid analysis were performed as described previously (Guillas *et al*., 2000; Fujita *et al*., 2006a).

Lipid Analysis

The lipids were analyzed by thin-layer chromatography (TLC) on a Silica gel 60 plate (Merck, Darmstadt, Germany) by using solvent system 1 (55:45:10, vol/vol $CHCl_3$:CH_3OH:0.25% KCl) or solvent system 2 (10:10:3, vol/vol $CHCl_3$:CH_3OH:H_2O). Reaction products separated on TLC plates were detected by autoradiography and analyzed using a Molecular Imager FX (Bio-Rad, Hercules, CA).

Radiolabeling of Proteins

Radiolabeling of proteins with [^{3}H]DHS (American Radiolabeled Chemicals, St. Louis, MO) was performed as described previously with some modifications (Guillas *et al*., 2000; Umemura *et al*., 2003).

Labeling of ceramide-containing proteins with [^{3}H]DHS was performed after cells were grown to the exponential phase in SC medium. Washed cells were resuspended in fresh SC medium containing 40 μg/ml myriocin (Sigma-Aldrich, St. Louis, MO), incubated at 30°C for 20 min, and incubated with [^{3}H]DHS for 2 h. The labeling reaction was stopped by adding cycloheximide, and cells were washed with 10 mM NaN_3. Labeled proteins were extracted by shaking with glass beads in TEPI buffer (100 mM Tris-HCl, pH 7.5, containing protease inhibitor cocktail; Roche, Mannheim, Germany), and solubilized by boiling in 1% SDS. Samples were combined with concanavalin A (Con A) buffer (50 mM Tris-HCl, pH 7.5, 150 mM NaCl, 1 mM $CaCl_2$, 1 mM $MnCl_2$,

and 1% Triton X-100) and centrifuged for 13,000 × *g*. Con A-Sepharose (GE Healthcare, Piscataway, NJ) was added to the supernatants, and the mixture was incubated overnight at 4°C to concentrate glycoproteins. The Sepharose beads were washed with Con A buffer and resuspended in SDS sample buffer. The samples were separated by SDS-polyacrylamide gel electrophoresis (PAGE) and analyzed using a Molecular Imager FX (Bio-Rad).

Preparation of Cell Lysate and Immunoblotting

Cells were grown to the exponential phase and collected by centrifugation. The cells were washed and broken using glass beads in TNPI buffer (50 mM Tris-HCl, pH 7.5, 150 mM NaCl, protease inhibitor cocktail [Roche], and 1 mM phenylmethylsulfonyl fluoride) at 4°C. Cell debris was removed by centrifugation. The cell extracts were then centrifuged at 13,000 × *g* to sediment the ER-rich fraction. The ER-rich pellet was solubilized in 1% Triton X-100 at 4°C for 30 min, and then it was centrifuged again at 13,000 × *g*. The supernatant was collected, mixed with SDS sample buffer, separated by SDS-PAGE, and analyzed by immunoblotting by using one of the following antibodies: anti-HA monoclonal antibody (mAb) 16B12 (1:2000; Cell Signaling Technology, Danvers, MA), anti-FLAG mAb M2 (1:10,000; Sigma-Aldrich), anti-Gas1 peptide polyclonal antibody (1:2000; kindly provided by Dr. Katsura Hata, Eisai, Tokyo, Japan), or anti-Dpm1p mAb (1:2000; Cell Signaling Technology).

Isolation of DRMs

Cells were grown at 30°C in YPAD to the exponential phase, and 3×10^8 cells were collected. DRMs for the Gas1p analysis were isolated as described previously with a slight modification (Bagnat *et al*., 2000; Okamoto *et al*., 2006). After incubation with 1% Triton X-100 for 30 min on ice, the lysates were subjected to OptiPrep density gradient floatation by centrifugation for 2 h at 40,000 rpm in a SW55Ti rotor (Beckman Coulter, Fullerton, CA). After centrifugation, six fractions of equal volume were collected starting from the top. Each fraction was mixed with sample buffer and subjected to SDS-PAGE and immunoblotting.

Immunoprecipitation

Immunoprecipitation was performed as described previously with some modifications (Rayner and Munro, 1998). The cells were grown to the exponential phase in YPAD, and then they were collected by centrifugation and washed with water. The washed cells were resuspended in Tris-Sorb buffer (1 M sorbitol, 50 mM Tris-HCl, pH 7.5) containing Zymolyase 100T (Seikagaku, Tokyo, Japan), and then they were incubated at 30°C for 30 min. The resulting spheroplasts were washed in Tris-Sorb buffer and lysed at 4°C for 30 min by gentle mixing in TNPI buffer. Next, the lysate was solubilized with 1% digitonin. Cell debris was removed by centrifugation, and the supernatant was incubated overnight with anti-FLAG M2 affinity gel (Sigma-Aldrich) or anti-HA affinity matrix (Roche). The beads were washed with TNPI buffer containing 1% digitonin and suspended into TNPI buffer containing 3xFLAG peptide (Sigma-Aldrich) or HA peptide (Roche) to elute the protein. The eluted proteins were denatured with SDS sample buffer, separated by SDS-PAGE, and analyzed by immunoblotting.

RESULTS

CWH43 Is a Homologue of Mammalian PGAP2 That Is Involved in GPI Lipid Remodeling

Recently, rat PGAP2 was reported to be a Golgi/ER resident membrane protein that seems to participate in the transfer of a saturated acyl chain to the *sn*-2 position of lyso-PI of the GPI anchor after the removal of the unsaturated acyl chain (Tashima *et al*., 2006). To further investigate lipid remodeling in yeast, we searched for the homologue of PGAP2 in *S. cerevisiae* by using BLAST (Altschul *et al*., 1997). The BLAST search revealed that the yeast homologue of PGAP2 is Cwh43p, a 953-amino acid protein that contains 18 potential membrane-spanning regions according to SOSUI analysis (Hirokawa *et al*., 1998). The amino acid sequence of human PGAP2 shares 24% homology with yeast Cwh43p; however, Cwh43p has an extra ~700-amino acid C terminus containing several membrane-spanning regions. This additional C-terminal extra part of Cwh43p is 31% identical to the product of an uncharacterized human gene, *FLJ21511* (Pittet and Conzelmann, 2007). Furthermore, it has been reported that *CWH43* is involved in the cell wall integrity (Martin-Yken *et al*., 2001). Therefore, we expected that Cwh43p participates in GPI lipid remodeling but that it also has some additional functions that are not shared by mammalian PGAP2.

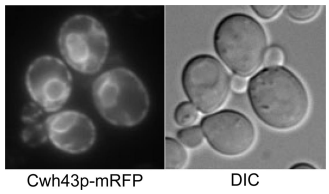

Figure 1. Cwh43p is localized in the ER. The localization of mRFP-tagged Cwh43p in *cwh43*Δ cells harboring pRS316T-CWH43-mRFP plasmid. The cells were cultured overnight at 30°C, and Cwh43p-mRFP was visualized by fluorescence microscopy. DIC, differential interference contrast.

Cwh43p Is an ER Resident Membrane Protein

We first constructed C-terminally green fluorescent protein (GFP)-tagged or mRFP-tagged *CWH43* expression plasmids to determine the intracellular location of Cwh43p. Both *CWH43-GFP* and *CWH43-mRFP* rescued the Calcofluor white (CFW) sensitivity of *cwh43* gene-disrupted cells (*cwh43*Δ), indicating that the tagged Cwh43 proteins were fully functional. Microscopic analysis indicated that Cwh43p-mRFP was mainly present in an intracellular perinuclear region with characteristics of the ER (Figure 1). Both Cwh43p-GFP and Cwh43p-mRFP were also localized at the intracellular perinuclear region. Moreover, according to the *Saccharomyces* Genome Database (SGD; http://www.yeastgenome.org/), GFP-fused Cwh43 protein is localized in the ER. Collectively, these results indicate that Cwh43p is localized in the ER. This is consistent with the previous report that Per1p and Gup1p, which are involved in GPI lipid remodeling, are also localized in the ER (Fujita *et al*., 2006a).

cwh43-disrupted Cells Show Sensitivity to CFW and High Temperature

Next, we characterized the phenotype of *cwh43*Δ cells. Disruption of *PER1* and *GUP1* (*per1*Δ and *gup1*Δ cells, respectively), which are involved in lipid remodeling of the GPI anchor, were sensitive to CFW, and they showed slow growth at 37°C (Bosson *et al*., 2006; Fujita *et al*., 2006a). The *cwh43*Δ cells also showed CFW sensitivity and temperature sensitivity at 39°C (Figure 3, vector) as reported previously (Martin-Yken *et al*., 2001), suggesting that they have a defect in cell wall integrity. The CFW sensitivity and temperature sensitivity of *cwh43*Δ cells were weaker than those of *per1*Δ and *gup1*Δ cells. These results imply that *CWH43* plays a different role in lipid remodeling than *PER1* and *GUP1*.

CWH43 Is Involved in Lipid Remodeling of the GPI Anchor from a Diacylglycerol- to a Ceramide Type

To address whether *CWH43* is also involved in the lipid remodeling of GPI anchor, we examined PI moieties obtained from GPI-anchored proteins of *cwh43*Δ cells. Cells were labeled with [^{3}H]inositol, and the protein pellet was delipidated. The solubilized glycoproteins were then concentrated by Con A-Sepharose and digested with pronase. The PI moieties were liberated from GPI anchors by nitrous acid deamination, and the purified PI moieties were then separated by TLC and detected by autoradiography (Figure 2A) (Guillas *et al*., 2000). In wild-type cells, PI moieties of GPI anchor are mainly inositolphosphorylceramide/B (IPC/B), which consists of PHS and C26:0 fatty acid, and pG1, which consists of PI containing a C26:0 fatty acid at the *sn*-2 position. The PI moieties of the GPI anchor in *gup1*Δ, *per1*Δ, and *gpi7*Δ cells were used as controls to identify the PI species. As reported previously (Bosson *et al*., 2006), the

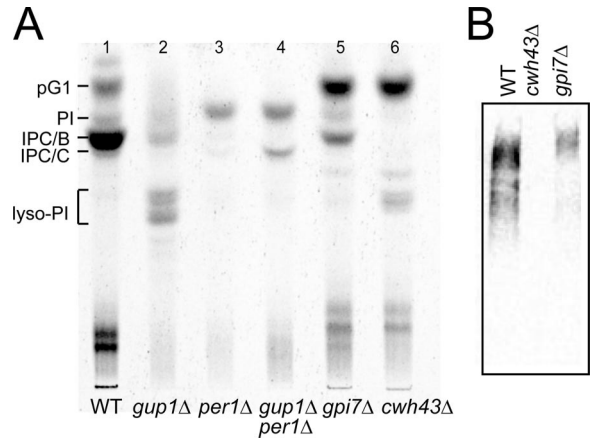

Figure 2. Lipid remodeling of lipid moieties in GPI anchors to ceramides is defective in *cwh43*Δ cells. (A) Analysis of PI moieties obtained from GPI-anchored proteins in wild-type (WT), *per1*Δ, *gup1*Δ, *per1*Δ*gup1*Δ, *gpi7*Δ, and *cwh43*Δ cells. Cells were labeled with [^{3}H]inositol at 30°C. Cell lysate was delipidated, and glycoproteins were concentrated using Con A-Sepharose. PI moieties of GPI anchors were released by deamination by using nitrous acid, separated by TLC by using solvent system 1, detected by autoradiography, and analyzed using a Molecular Imager FX. (B) Analysis of incorporation of [^{3}H]DHS derivatives in proteins. Cells were incubated for 20 min in the presence of myriocin and then labeled with [^{3}H]DHS at 30°C. Glycoproteins were concentrated from extracted lysate using Con A-Sepharose and separated by SDS-PAGE. Radiolabeled proteins were visualized using a Molecular Imager FX. Equal loading of total proteins was confirmed by Coomassie brilliant blue staining of the SDS-PAGE gels.

*gup1*Δ cells, which have a defect in acylation of lyso-PI at the *sn*-2 position, accumulated lyso-PI (Figure 2A, lane 2), and the *per1*Δ cells, which have a defect in GPI-PLA$_2$, accumulated PI containing short-chain fatty acid (Fujita *et al*., 2006a; Figure 2A, lane 3). In *gpi7*Δ cells, lipid remodeling in Golgi is defective, resulting in a lack of IPC/C in the GPI anchor (Benachour *et al*., 1999). As reported, IPC/B was decreased, whereas pG1 was increased in *gpi7*Δ cells (Figure 2A, lane 5). The *cwh43*Δ cells accumulated pG1 and lyso-PI (Figure 2A, lane 6). We detected neither IPC/B nor IPC/C species of GPI anchor in *cwh43*Δ cells, suggesting that the *cwh43*Δ cells have a defect in the lipid remodeling of the GPI anchor from a diacylglycerol type to a ceramide type.

To confirm the aforementioned result that the lipid moiety of GPI-anchored proteins dose not contain ceramides, we examined the incorporation of [^{3}H]DHS into proteins. When endogenous DHS biosynthesis is blocked by myriocin (Horvath *et al*., 1994), exogenous [^{3}H]DHS is converted to ceramides, and the [^{3}H]DHS-derived ceramides are incorporated into the remodeled, ceramide-containing GPI-anchored proteins (Reggiori *et al*., 1997). Cells were labeled with [^{3}H]DHS, and total lysates were extracted. In wild-type cells, the ^{3}H signal derived from DHS was clearly detected in GPI-anchored proteins, whereas the amount of ^{3}H incorporation was reduced in *gpi7*Δ cells (Figure 2B) as reported previously (Benachour *et al*., 1999). Conversely, we did not detect any incorporation of ^{3}H into remodeled GPI-anchored proteins in *cwh43*Δ cells, indicating that the lipid moieties of GPI-anchored proteins were not remodeled to ceramide. These results strongly suggest that *CWH43* is involved in the lipid remodeling of ceramide-containing GPI anchors after the transfer of GPI to proteins.

The accumulation of pG1 in *cwh43*Δ cells might be caused by a defect in sphingolipid biosynthesis. To check whether the sphingolipid biosynthesis is defective, we examined the accumulation of inositolphosphorylceramides (IPCs). The *cwh43*Δ cells have similar amounts of inositolphosphorylceramide, mannose inositolphosphorylceramide, and mannose diinositolphosphorylceramide as wild-type cells (unpublished data). This result suggests that the biosynthesis of ceramide and sphingolipid is normal in *cwh43*Δ cells and that the defect in the lipid remodeling of diacylglycerol to ceramide in *cwh43*Δ cells is not caused by a defect in ceramide biosynthesis.

We further analyzed the localization of a major GPI-anchored protein, Gas1p, to investigate whether GPI-anchored proteins have a defect in *cwh43*Δ cells. First, we compared the amount of Gas1p in the wild-type and *cwh43*Δ cells. Total cell lysates were examined by immunoblotting with an anti-Gas1 antibody. In contrast to wild-type cells, Gas1p was drastically reduced in *per1*Δ and *gup1*Δ cells, and, in turn, released to the medium (Supplemental Figure S1A), as reported previously (Fujita *et al*., 2006a). Alternatively, in *cwh43*Δ cells, the level of Gas1p in cell lysates was not decreased, and it was not released into the medium, indicating that Gas1p is almost retained normally in *cwh43*Δ cells. Next, we analyzed the cellular localization of mRFP-tagged Gas1p in wild-type and *cwh43*Δ cells by fluorescence microscopy. In *cwh43*Δ cells, mRFP-Gas1p was localized at the cell surface in the same manner as in wild-type cells (Supplemental Figure S1B), indicating that the localization of Gas1p is not affected in *cwh43*Δ cells.

It is reported that Gas1p is incorporated into lipid rafts at the plasma membrane (Bagnat *et al*., 2000). Therefore, we checked whether Gas1p is sorted to the DRM in *cwh43*Δ cells. In *cwh43*Δ cells, Pma1p, a marker for DRM-associated membrane protein, was associated with the DRMs, indicating that raft formation itself was normal (Supplemental Figure S1C). In the wild-type and *cwh43*Δ cells, Gas1p was also located predominantly in the DRM fraction, suggesting that Gas1p in *cwh43*Δ cells is located in lipid rafts as in wild-type cells, different from that in *per1*Δ or *gup1*Δ cells. It has been reported that the lipid moiety of GPI anchor of Gas1p is a diacylglycerol type containing a C26 fatty acid (Fankhauser *et al*., 1993). Therefore, it is possible that the lipid moiety of Gas1 could be normal and localization of Gas1p is not affected in *cwh43*Δ cells, consisting with the aforementioned results that *CWH43* is involved in the lipid remodeling of GPI anchor to ceramides.

The C-Terminal Domain of Cwh43p Is Essential for Lipid Remodeling to Ceramide

Although the N-terminal region of Cwh43p (Cwh43-N) is homologous to mammalian PGAP2, Cwh43p has a large C-terminal region (Cwh43-C) that is similar to an uncharacterized gene product encoded by human *FLJ21511*. Therefore, Cwh43p corresponds to a fusion of PGAP2 and FLJ21511 proteins. To investigate which region of Cwh43p is important for its function, we constructed plasmids for expressing both *CWH43-N* (encoding amino acids 1-229; 229 amino acids) and *CWH43-C* (encoding amino acids 218-953; 736 amino acids). The proteins produced by these expression plasmids, Cwh43-N and Cwh43-C, are tagged with three copies of the HA epitope at their C termini. Furthermore, these expression plasmids were under control of the *CWH43* promoter. These two plasmids were referred to as pRS316T-CWH43-N-HA and pRS316T-CWH43-C-HA, respectively. The expression plasmids were introduced into *cwh43*Δ cells, and the phenotypes of the *cwh43*Δ cells harboring them were characterized (Figure 3). The *cwh43*Δ cells harboring the empty vector were CFW and temperature sensitive, and these sensitivities were rescued by introduction of *CWH43*

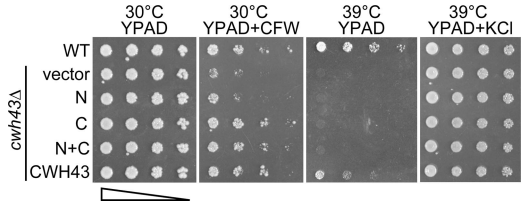

Figure 3. *CWH43-C* but not *CWH43-N* rescues the CFW sensitivity of *cwh43*Δ cells. *CWH43-C* partially suppresses the phenotype of *cwh43*Δ cells. Serial dilutions (4-fold) of cells were spotted on YPAD, YPAD containing 10 μg/ml CFW, or YPAD containing 0.3 M KCl and then incubated for 2 d at 30 or 39°C.

gene. The *cwh43*Δ cells harboring the *CWH43-N* expression plasmid were also CFW and temperature sensitive. Although the CFW sensitivity of *cwh43*Δ cells was rescued by the *CWH43-C* expression plasmid alone or both the *CWH43-C* and *CWH43-N* expression plasmids, they did not rescue the temperature sensitivity of *cwh43*Δ cells (Figure 3). All cells were able to grow on YPAD plates containing 0.3 M KCl, indicating that cells with high temperature sensitivity also have a defect in the cell wall. These results suggest that *CWH43-C* partially suppresses the phenotype of *cwh43*Δ cells.

To analyze lipid remodeling of GPI in *CWH43-N*– and *CWH43-C*–introduced *cwh43*Δ cells, we further constructed plasmids for expressing *CWH43*, *CWH43-N*, and *CWH43-C* and whose expression is under control of the constitutive *S. cerevisiae TDH3* promoter, generating YEp352GAPII-CWH43-HA, YEp352GAPII-CWH43-N-HA, and YEp352GAPII-CWH43-C-HA, respectively. The plasmids were introduced into *cwh43*Δ cells, and the expression of the Cwh43-HA, Cwh43-N-HA, and Cwh43-C-HA proteins was confirmed by immunoblotting by using an anti-HA antibody. The cells were grown to the exponential phase, and then they were broken by vigorous mixing with glass beads. The ER-rich fraction was concentrated by centrifugation for 13,000 × *g* and then solubilized with Triton X-100. The proteins were separated by SDS-PAGE and analyzed by immunoblotting with an anti-HA antibody. We detected Cwh43-HA protein, Cwh43-N-HA protein, and Cwh43-C-HA proteins at 100, 25, and 75 kDa, respectively, consistent with their estimated molecular masses (Figure 4A).

Next, we analyzed PI moieties obtained from GPI-anchored proteins by deamination. In the *cwh43*Δ cells harboring the *CWH43* expression plasmid, the lipid moieties of GPI anchors were mainly IPC/B (Figure 4B, lane 2), and in *cwh43*Δ cells harboring the empty vector, the PI moieties were mainly pG1, a PI containing C26:0 fatty acid at the *sn*-2 position (Figure 4B, lane 3), as described above. The *cwh43*Δ cells harboring the *CWH43-N* expression plasmid (*CWH43-N* cells) accumulated pG1, as observed in the *cwh43*Δ cells (Figure 4B, lane 5). In contrast, the *cwh43*Δ cells harboring the *CWH43-C* expression plasmid (*CWH43-C* cells) accumulated a small but significant amount of IPC/B in addition to pG1 and lyso-PI (Figure 4B, lane 4), suggesting that the C-terminal region of Cwh43p is important for its ability to remodel lipids to ceramides. In addition, the *cwh*43Δ cells coexpressed both *CWH43-N* and *CWH43-C* (*CWH43-N/C* cells) accumulated more IPC/B than the cells expressed *CWH43-C* alone (Figure 4B, lane 6), indicating that *CWH43-N* is able to enhance the lipid remodeling to ceramides by *CWH43-C*.

To confirm that *CWH43-C* is important for the remodeling of GPI anchors to ceramides, we further examined the incorporation of [^{3}H]DHS derivatives into proteins in *CWH43-C*–expressing cells. The cells were labeled with [^{3}H]DHS, and cell lysates were prepared. Glycoproteins were concentrated with Con A-Sepharose, and they were separated by SDS-PAGE. In *cwh43*Δ cells harboring the *CWH43* expression plasmid, [^{3}H]labeled DHS derivatives were incorporated into proteins, whereas the incorporation of ^{3}H-labeled

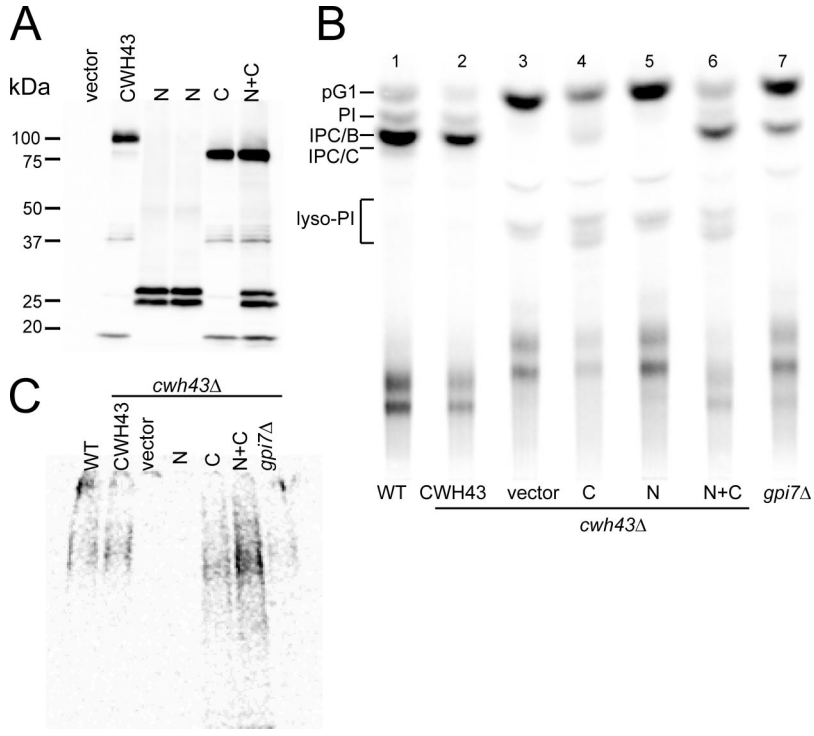

Figure 4. The C-terminal domain of Cwh43p is essential for lipid remodeling to ceramides. (A) Expression of *CWH43-HA*, *CWH43-C-HA*, and *CWH43-N-HA* was confirmed by immunoblotting by using an anti-HA antibody. The *cwh43*Δ cells harboring the *CWH43-HA* (CWH43), *CWH43-N-HA* (N), and *CWH43-C-HA* (C) expression plasmids, respectively, and *cwh43*Δ cells harboring both *CWH43-N-HA* and *CWH43-C-HA* expression plasmids (N+C) were cultured at 30°C. The lysates were extracted, and ER-rich fractions were concentrated by centrifugation at 13,000 × *g* and separated by SDS-PAGE. (B) Analysis of PI moieties obtained from GPI anchor in wild-type (WT), *gpi7*Δ, and *cwh43*Δ cells harboring *CWH43*, *CWH43-N* (N), *CWH43-C* (C), and both *CWH43-N* and *CWH43-C* (N+C) expression plasmids. Cells were labeled with [^{3}H]inositol. PI moieties obtained from delipidated glycoproteins by deamination were analyzed by TLC as described in Figure 2A. (C) Cells were labeled with [^{3}H]DHS in the presence of myriocin. The incorporation of [^{3}H]DHS derivatives into proteins in the same cells as shown in Figure 4B was analyzed as described in Figure 2B.

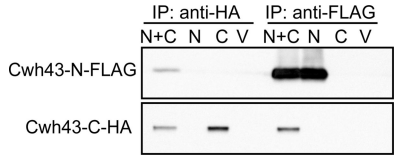

Figure 5. Cwh43-N associates with Cwh43-C. The *cwh43*Δ cells introduced with both *CWH43-N* and *CWH43-C* plasmids (N+C), both *CWH43-N* plasmid and empty vector (N), both *CWH43-C* plasmid and empty vector (C), and two empty vectors (V) were cultured at 30°C. Total cell lysates solubilized with digitonin were immunoprecipitated using FLAG-beads or HA-beads. The immunoprecipitated samples were separated by SDS-PAGE and analyzed by immunoblotting using an anti-FLAG antibody or an anti-HA antibody.

DHS derivatives was scarcely detected in *cwh43*Δ cells harboring the empty vector (Figure 4C). In contrast, in *CWH43-C* cells but not *CWH43-N* cells, ^{3}H-labeled DHS derivatives were incorporated into proteins. Moreover, in *CWH43-N/C* cells, there was a higher level of incorporation than in *CWH43-C* cells. These results suggest that the C-terminal region of Cwh43p is important for GPI lipid remodeling from the diacylglycerol type to the ceramide type and that the N-terminal region of Cwh43p enhances ceramide formation by the C-terminal region. Therefore, we designated these N- and C-terminal regions of Cwh43p as Cwh43-N and Cwh43-C domains, respectively.

The Cwh43-N Domain Associates with the Cwh43-C Domain

Because *CWH43-N* enhanced the function of *CWH43-C*, we suspected that Cwh43-N protein associates with Cwh43-C protein. To test this possibility, we performed a coimmunoprecipitation assay. Cwh43-N was tagged at its C terminus with three copies of FLAG epitope (encoded by *CWH43-N-FLAG* gene). *CWH43-N-FLAG* and *CWH43-C-HA* were coexpressed from the *CWH43* promoter in yeast cells, and the products were immunoprecipitated from total lysates solubilized by mild detergent treatment with digitonin. Cwh43-N-FLAG was immunoprecipitated with FLAG-beads, and Cwh43-C-HA was immunoprecipitated with HA-beads. The immunoprecipitates were separated by SDS-PAGE and examined by immunoblotting. Cwh43-N-FLAG was coprecipitated with Cwh43-C-HA and Cwh43-C-HA with Cwh43-N-FLAG when the two were coexpressed but not in control samples (Figure 5). These results demonstrate that domains Cwh43-N and Cwh43-C associate with each other.

A Highly Conserved Region of Cwh43-C Domain Is Important for the Lipid Remodeling Function

As described previously (Martin-Yken *et al*., 2001), we found that the *cwh43-2* mutant, in which a conserved glycine at amino acid 57 was replaced with arginine (G57R), is CFW sensitive and that it reduced cell wall integrity (Figure 6A), but why the mutant is sensitive to CFW and whether G57 is essential for the remodeling activity of Cwh43p has not been determined. To examine the GPI phenotypes in the *cwh43-2* mutant, we constructed a plasmid for expressing G57R-mutated Cwh43-HA and introduced it into *cwh43*Δ cells. Analysis of the PI moieties obtained from GPI-anchored protein revealed that IPC/B was greatly reduced in the *cwh43-2* mutant compared with cells expressing the wild-type Cwh43p (Figure 6D, lanes 1 and 2). The amount of Cwh43-G57R-HA protein was also lower than in wild-type Cwh43p (Figure 6C, lanes 1 and 2). These results suggest that an intracellular decrease in Cwh43p causes a defect in lipid remodeling to ceramides. Together, these findings suggest that the G57R substitution causes instability in the Cwh43 protein, resulting in a decrease in Cwh43p function.

We next tried to identify the other amino acids that are important for Cwh43p function (i.e., lipid remodeling of diacylglycerol to ceramides). We focused on the C-terminal domain of Cwh43p because it is essential for the remodeling of Cwh43p. We constructed several C-terminal mutants of *CWH43*. Based on the amino acid alignment of Cwh43-C and its homologues in fission yeast, fungi, mouse, and human, we substituted conserved residues H472, D693, H770/H771, E807, D862, R882 with alanine in Cwh43-C (Figure 6B). The mutant *CWH43-C*–expressing plasmids were introduced into *cwh43*Δ cells, and the expression of the mutant proteins was confirmed by immunoblotting by using an anti-HA antibody. The amounts of these mutant Cwh43-C proteins were similar to that of wild-type Cwh43-C (Figure 6C).

Next, we characterized the PI moieties obtained from the GPI-anchored proteins produced by these mutant cells (Figure 6D). Wild-type *CWH43-C*–introduced *cwh43*Δ cells accumulated a small amount of IPC/B in addition to pG1 and lyso-PI, whereas *cwh43*Δ cells harboring the empty vector accumulated pG1 and lyso-PI but not IPC/B (Figure 6D), as described above. Interestingly, in R882A mutant *cwh43-C*–introduced *cwh43*Δ cells, IPC/B lipid moieties were not detected in GPI anchor (Figure 6D, lane 9). Also, the amount of IPC/B was decreased in D862A mutant *cwh43-C*–introduced *cwh43*Δ cells (Figure 6D, lane 8), whereas the amount of IPC/B was not decreased in the other mutant *cwh43-C*–introduced *cwh43*Δ cells. Furthermore, D862A and R882A mutants of *CWH43-C* did not complement the CFW sensitivity of *cwh43*Δ cells, whereas the sensitivity was complemented by the wild type and H472A, D693A, H770A/H771A, and E807A mutants of *CWH43-C* (Figure 6E). We also checked whether GPI-anchored proteins are remodeled to ceramide, which can be detected by incorporation of ^{3}H-labeled DHS derivatives into proteins in these mutant cells. In the *cwh43*Δ cells introduced with the R882A mutant *CWH43-C*, ^{3}H-labeled signals were not detected in proteins, whereas ^{3}H-labeled signals were observed in the other mutant and wild-type *CWH43-C*–introduced *cwh43*Δ cells (Figure 6F). The ^{3}H-labeled DHS derivatives were incorporated into proteins in D862A mutant *CWH43-C*–introduced *cwh43*Δ cells, implying that these mutant cells had a detectable amount of IPC/B in the PI moiety. These results suggest that R882 is an important amino acid residue for the lipid remodeling function and that the conserved region containing D862 and R882 is important for the function of Cwh43p, although the detailed mechanism is not clear.

The Mouse CWH43 Counterparts FRAG1 and C130090K23 Complement CWH43-deficient Yeast Phenotypes

According to a BLAST search, the mouse homologues of human *PGAP2* and *FLJ21511* are *FRAG1* and *C130090K23*, respectively. The predicted amino acid sequences of mouse FRAG1 and C130090K23 are 29 and 31% identical to yeast Cwh43p, respectively. To address whether mouse *C130090K23* is a functional homologue of *CWH43-C*, we introduced expression plasmids of *FRAG1* and *C130090K23* into the *cwh43*Δ cells and examined CFW sensitivity and PI moieties obtained from GPI-anchored proteins.

The *C130090K23* gene rescued the CFW sensitivity of *cwh43*Δ, but the *FRAG1* gene did not (Figure 7A). This is similar to the results for *CWH43-C*– and *CWH43-N*–introduced *cwh43*Δ cells, respectively (Figure 3). These results suggest that *C130090K23* but not *FRAG1* rescues the cell wall defect in *cwh43*Δ cells.

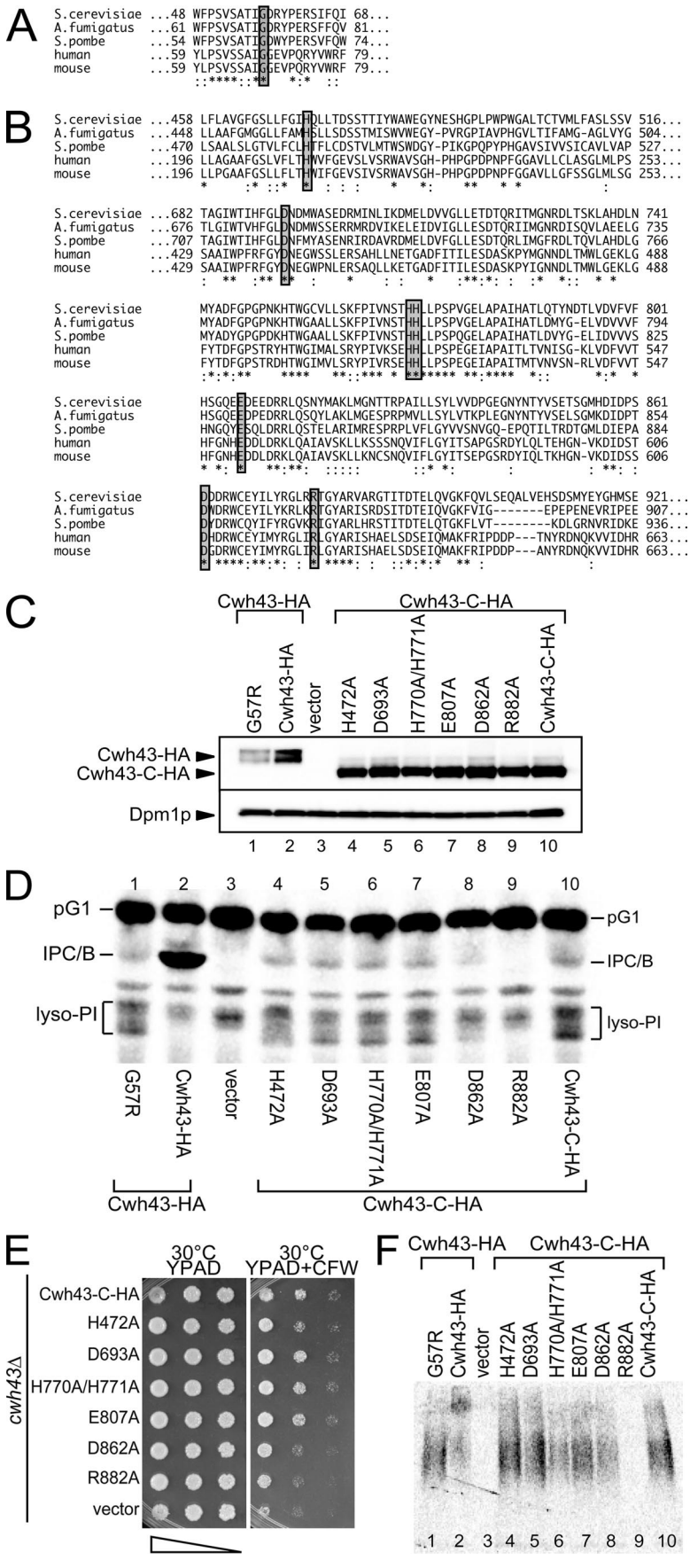

Figure 6. The highly conserved region containing D862 and R882 is essential for the function of Cwh43-C. (A) Alignment of the amino acid sequences of the highly conserved N-terminal region of Cwh43p containing G57. The amino acid sequences of *S. cerevisiae*, *Aspergillus fumigatus*, *Schizosaccharomyces pombe*, *Homo sapiens*, and *Mus musculus* proteins were aligned using ClustalW. Asterisks (*) and colons (:) indicate identical and conserved amino acids, respectively. (B) Alignment of the amino acid sequences of the highly conserved C-terminal region of Cwh43p containing H472A, D693A, H770A/H771A, E807A, D862A, R882A. The amino acid sequences of *S. cerevisiae*, *A. fumigatus*, *S. pombe*, *H. sapiens*, and *M. musculus* proteins were aligned using ClustalW. (C) The production of Cwh43-HA, G57R mutant Cwh43-HA, Cwh43-C-HA, and H472A, D693A, H770A/H771A, E807A, D862A, and R882A mutants of Cwh43-C-HA in *cwh43*Δ cells was examined by immunoblotting by using anti-HA and anti-Dpm1p antibodies. Cells were cultured at 30°C, and cell lysates were extracted. ER-rich fractions were concentrated by centrifugation at 13,000 × *g* and separated by SDS-PAGE. Dpm1p was used to confirm equal loading. (D) Analysis of PI moieties obtained from GPI-anchored protein by deamination in the same cell as shown in Figure 6C. Cells were labeled with [^{3}H]inositol, and PI moieties obtained from GPI-anchored proteins by deamination were analyzed as described in Figure 2A. (E) The same cells as in Figure 6C were analyzed for CFW sensitivity. The cells were cultured on YPAD and YPAD containing 10 μg/ml CFW at 30°C for 2 d as described in Figure 3. (F) Analysis of incorporation of [^{3}H]DHS derivatives into proteins in the same cells as in Figure 6C. Cells were labeled with [^{3}H]DHS in the presence of myriocin, and incorporation of [^{3}H]DHS was analyzed as described in Figure 2B.

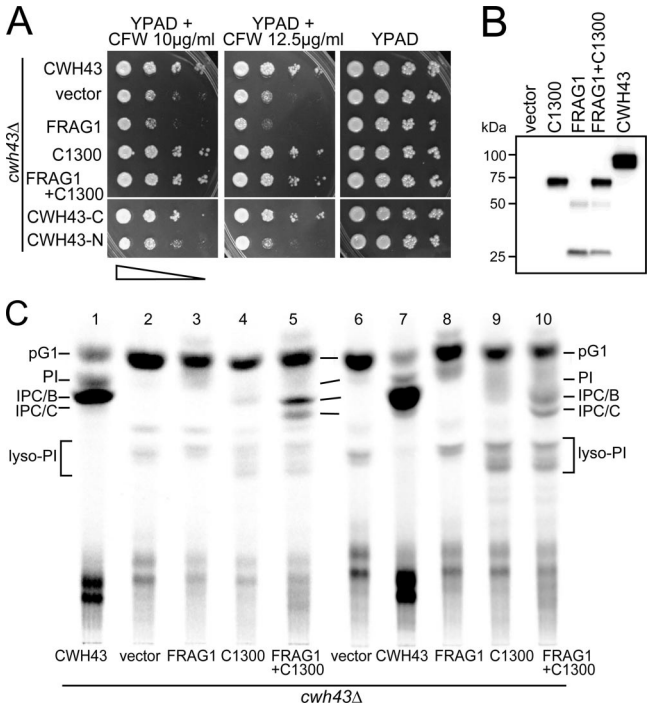

Figure 7. The mouse *C130090K23* gene suppresses the phenotype of yeast *cwh43*Δ cells. (A) The mouse *C130090K23* gene rescues the CFW sensitivity of *cwh43*Δ cells. *cwh43*Δ cells harboring *CWH43*, the empty vector (vector), *FRAG1*, *C130090K23* (C1300), both *FRAG1* and *C130090K23* (FRAG1+C1300), *CWH43-C*, and *CWH43-N* expression plasmids were cultured on YPAD and YPAD containing CFW at 30°C for 2 d as described in Figure 3. (B) The production of Cwh43-HA (CWH43), C130090K23-HA (C1300), FRAG1-HA (FRAG1), and both FRAG1-HA and C130090K23-HA (FRAG1+C1300) in *cwh43*Δ cells was confirmed by immunoblotting by using an anti-HA antibody as described in Figure 4A. (C) Mouse *C130090K23* recovers the function of GPI lipid remodeling to ceramides. PI moieties obtained from GPI-anchored proteins by deamination were analyzed in *cwh43*Δ cells harboring *CWH43*, the empty vector, *FRAG1*, *C130090K23* (C1300), and both *FRAG1* and *C130090K23* (FRAG1+C1300) as described in Figure 2A. The results from two independent experiments are shown in left (lanes 1–5) and right (lanes 6–10) panels, respectively.

To address whether C130090K23 can remodel PI moieties from diacylglycerol type to ceramides type, we analyzed the lipid moieties obtained from GPI-anchored proteins in *cwh43*Δ cells introduced with *C130090K23*. We first confirmed the production of C130090K23 and FRAG1 proteins in *cwh43*Δ cells by immunoblotting with an anti-HA antibody (Figure 7B). These proteins were designed to contain three copies of the HA epitope at their C termini. We detected the mouse FRAG1-HA and the mouse C130090K23-HA proteins as 25- and 75-kDa bands, respectively, consistent with their estimated molecular masses, although the expression level of the mouse proteins was lower than that of the yeast Cwh43-HA protein.

Next, we analyzed the lipid moieties of GPI-anchored proteins in *cwh43*Δ cells harboring *C130090K23* and *FRAG1*. The cells were labeled with [^{3}H]inositol, and the labeled glycoproteins were concentrated by Con A-Sepharose and digested with pronase. The PI moieties were obtained by deamination and were separated by TLC. In *cwh43*Δ cells harboring the *CWH43* gene, the PI moiety was mainly IPC/B, which consists of PHS and C26 fatty acid (Figure 7C, lanes 1 and 7), and in the *cwh43*Δ cells harboring the empty vector, the PI moieties were pG1, a PI with C26 fatty acid in the *sn*-2 position, and lyso-PI (Figure 7C, lanes 2 and 6), as described above. The *cwh43*Δ cells harboring *FRAG1* accumulated pG1 and lyso-PI like the *cwh43*Δ cells harboring the empty vector (Figure 7C, lanes 3 and 8). In contrast, the *cwh43*Δ cells harboring *C130090K23* accumulated a small but significant amount of IPC/B in addition to pG1 and lyso-PI (Figure 7C, lanes 4 and 9). Moreover, the *cwh43*Δ cells coexpressing *FRAG1* and *C130090K23* accumulated not only IPC/B but also IPC/C, which consists of PHS and a hydroxylated C26:0 fatty acid (Figure 7C, lanes 5 and 10). The level of IPC in *cwh43*Δ cells coexpressing *FRAG1* and *C130090K23* was higher than that of *cwh43*Δ cells expressing *C130090K23* alone, as observed in *cwh43*Δ cells coexpressing *CWH43-N* and *CWH43-C*. These results suggest that the mouse C130090K23 protein can remodel lipids of PI moieties in GPI-anchored proteins from diacylglycerol type to ceramides and that the independent mouse FRAG1 protein is able to enhance lipid remodeling to ceramides by C130090K23.

Because Cwh43-N and Cwh43-C associated with each other, we further investigated whether FRAG1 is coimmunoprecipitated with C130090K23. FRAG1 was tagged with three copies of the HA epitope at its C terminus (FRAG1-HA), and C130090K23 was tagged with three copies of FLAG epitope at its C terminus (C130090K23-FLAG). The tagged mouse genes were coexpressed under the constitutive *TDH3* promoter and introduced into *cwh43*Δ cells. The digitonin-solubilized total lysates of *cwh43*Δ cells coexpressing *FRAG1-HA* and *C130090K23-FLAG* were extracted, and FRAG1-HA and C130090K23-FLAG proteins were immunoprecipitated by HA-beads and FLAG-beads, respectively. FRAG1-HA coprecipitated with C130090K23-FLAG in lysates containing C130090K23-FLAG but not in control lysates (Figure 8A). C130090K23-FLAG also coprecipitated with FRAG1-HA in lysates containing FRAG1-HA. Because interaction of FRAG1-HA and C130090K23-FLAG are shown in low efficiency, we further tried the immunoprecipitation by using FRAG1-FLAG and C130090K23-HA. FRAG1-FLAG was coprecipitated with C130090K23-HA and C130090K23-HA with FRAG1-FLAG when the two were coexpressed but not in control sample. These results indicate that, like Cwh43-N and Cwh43-C, FRAG1 and C130090K23 associate with each other.

Moreover, we examined the association of C130090K23-FLAG and FRAG1-FLAG with Alg14-HA to exclude the possibility that the interaction is derived from some artifact. Alg14p, which is an ER-resident membrane protein, is associated with Alg13p and involved in $GlcNAc_2$-PP-dol formation (Bickel *et al*., 2005; Gao *et al*., 2005). ALG14-HA expressing plasmid was cointroduced with C130090K23-FLAG–, FRAG1-FLAG–, or ALG13-FLAG–expressing plasmids into *cwh43*Δ cells. Total lysate was immunoprecipitated using FLAG affinity agarose gels, and immunoprecipitation samples are analyzed by immunoblotting using anti-FLAG, anti-HA, and anti-Dpm1p antibodies. Alg13-FLAG was coimmunoprecipitated with Alg14-HA, but not with FRAG1-FLAG and C130090K23-HA. Moreover, in all three immunoprecipitation samples, Dpm1p was not detected as any distinct bands, although Dpm1p was detected in total lysate of all three samples. These results suggest that C130090K23-FLAG and FRAG1-FLAG are not physically interacted with Alg14p-HA and Dpm1p. Together, C130090K23 and FRAG1 are specifically associated together.

DISCUSSION

The lipid remodeling of yeast GPI-anchored protein begins with the removal of an unsaturated fatty acyl chain from diacylglycerol by a GPI-PLA_2 activity. Per1p is involved in this reaction (Fujita *et al*., 2006a). Next, a saturated long fatty

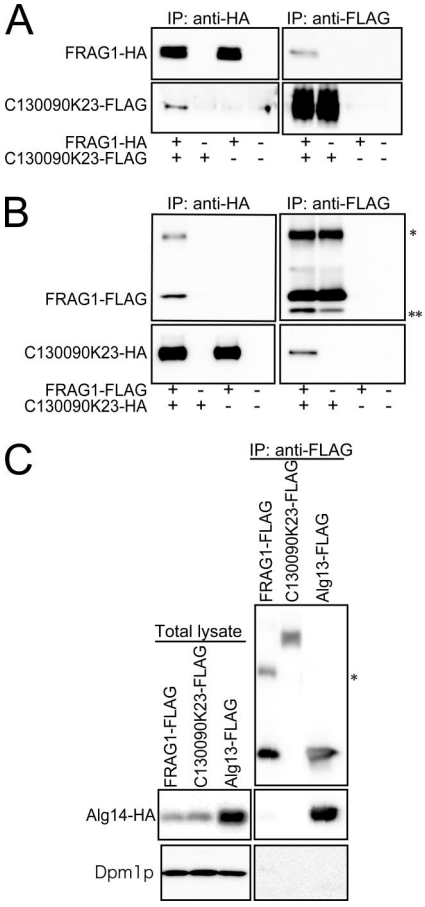

Figure 8. Mouse FRAG1 and C130090K23 proteins associate with each other. (A) The *cwh43*Δ cells harboring *FRAG1-HA* and *C130090K23-FLAG* expression plasmids or the empty vector were cultured at 30°C. Total cell lysates were extracted with digitonin, immunoprecipitated, and analyzed by immunoblotting as described in Figure 5. (B) *cwh43*Δ cells harboring *FRAG1-FLAG* and *C130090K23-HA* expression plasmids or the empty vector were used for immunoprecipitation as described in Figure 8A. We think that the upper bands of FRAG1-FLAG (*) may be dimmer form and the lower bands of FRAG1-FLAG (**) may be degradation form. (C) *cwh43*Δ cells coexpressed *ALG14-HA* with *FRAG1-FLAG*, *C130090K23-FLAG* and *ALG13-FLAG* were cultured at 30°C. Total lysates were extracted, immunoprecipitated using FLAG-beads, and analyzed immunoblotting with anti-FLAG, anti-HA, and anti-Dpm1p antibodies.

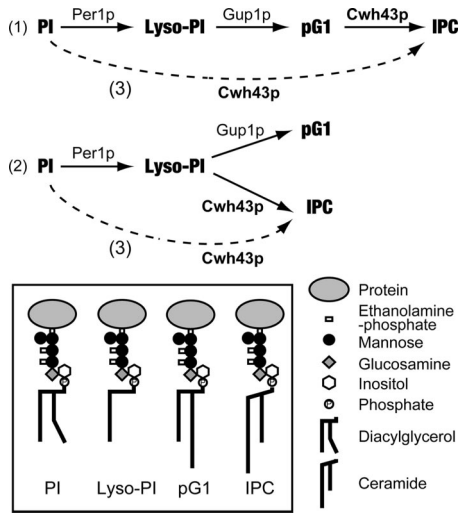

Figure 9. The hypothetical lipid remodeling pathways of GPI-anchored proteins in yeast. These three pathways [(1), (2), and (3)] of GPI lipid remodeling are proposed based on our results and previous reports (Sipos *et al*., 1997; Bosson *et al*., 2006; Fujita *et al*., 2006a), as described in *Discussion*. The first possible pathway (1) is sequential, and the second pathway (2) is diverged, and there also might be a bypass (3) for these pathways. Our current studies indicate that Cwh43p is required to form IPC of lipid moiety in GPI-anchored proteins.

acyl chain is transferred to lyso-GPI by the *O*-acyltransferase Gup1p (Bosson *et al*., 2006), generating diacylglycerol containing a C26 fatty acid. Most mature GPI-anchored proteins, however, contain ceramides in their lipid moieties. Our analysis of the lipid moiety obtained from GPI-anchored proteins by deamination showed that *cwh43*Δ cells accumulate pG1, which is a PI containing a saturated C26 fatty acid, and lyso-PI but not IPCs. Therefore, it is conceivable that *CWH43* is involved in the remodeling of GPI-anchored proteins from the diacylglycerol type to the ceramide type.

On the basis of our results and previous reports (Sipos *et al*., 1994; Bosson *et al*., 2006; Fujita *et al*., 2006a), we speculated that there are two possibilities for the remodeling pathway of GPI lipids to ceramides (Figure 9). One possibility may be a sequential pathway and the other may be diverged pathway. In former case [Figure 9, (1)] an unsaturated fatty acid is removed from diacylglycerol of conventional PI to generate lyso-PI-type GPI anchor (lyso-PI). Per1p is involved in this process. Next, a C26 saturated fatty acid is transferred to lyso-PI by the *O*-acyltransferase Gup1p, generating PI with diacylglycerol containing a C26 saturated fatty acid at the *sn*-2 position (pG1). Diacylglycerol containing a C26 saturated fatty acid may then be converted to a ceramide moiety (IPC). Cwh43p may be involved in this step because the GPI-anchored proteins from *cwh43*Δ cells accumulated pG1-type PI. Alternatively, the pathway may diverge. In this case, the lyso-PI generated by Per1p could be used as a substrate for two reactions executed by Gup1p and Cwh43p [Figure 9, (2)]. In one of these reactions, C26 saturated fatty acid is transferred to lyso-PI by Gup1p to generate diacylglycerol containing a C26 fatty acid (pG1). In the other reaction, lyso-PI may be substituted directly for ceramide moiety (IPC), a step that may involve Cwh43p. In this case, the pathway where lyso-PI is transferred with C26 fatty acid to generate diacylglycerol might be enhanced when the conversion to ceramides is defective. A third additional pathway may also exist as an option of both sequential and diverged pathways, as shown by dotted lines in Figure 9 (3). Diacylglycerol with an unsaturated fatty acid in conventional PI is directly exchanged for a ceramide moiety, together with the pathway mediated by Per1p and Gup1p. Cwh43p could be involved in this direct exchange of unsaturated fatty acid for a ceramide moiety because GPI-anchored proteins from *per1*Δ*gup1*Δ double-mutant cells accumulate IPC/C in addition to PI (Fujita *et al*., 2006a). This third alternative may operate as a bypass or as an emergency route for exchange when there is a defect in the steps mediated by Per1p and Gup1p. Identification of a direct substrate for Cwh43p should help determine the detailed molecular mechanism of lipid remodeling in GPI anchors to ceramides.

We found that the plasma membrane localization of a major GPI-anchored protein, Gas1p, was unaffected in *cwh43*Δ cells, whereas other studies have shown that Gas1p

is released into the medium in *per1*Δ and *gup1*Δ cells (Bosson *et al*., 2006; Fujita *et al*., 2006a). It has been reported that the lipid moiety of GPI anchor to which Gas1p is attached is a diacylglycerol type containing a C26 fatty acid (Fankhauser *et al*., 1993). Therefore, it is possible that the lipid moiety of Gas1 could be a diacylglycerol type even in *cwh43*Δ cells, which is consistent with the finding that the localization of Gas1p was unchanged in *cwh43*Δ cells. Except for Gas1p, specific GPI-anchored proteins predominantly containing ceramide in the lipid moiety have not been identified in *S. cerevisiae*, even though they more often contain ceramide-type than diacylglycerol-type lipid moieties (Sipos *et al*., 1997). Thus, it is likely that unknown GPI-anchored proteins containing ceramide in their lipid moieties might be affected in *cwh43*Δ cells. Because phenotype of Gas1p localization and the association of Gas1p with DRM in *cwh43*Δ cells was weaker than in *per1*Δ and *gup1*Δ cells, it is possible that the diacylglycerol-type lipid moiety of GPI anchors may be sufficient for correct association with the lipid microdomain even in *cwh43*Δ cells.

Moreover, the *cwh43*Δ cells introduced with *CWH43-C* are able to produce GPI anchor containing IPC/B, suggesting that C-terminal domain is essential for the ability to remodel GPI lipids ceramides. The function of *CWH43-C* was enhanced when coexpressed with *CWH43-N*. Furthermore, the G57R mutant of Cwh43p was unstable, and a much smaller amount of GPI-anchor–derived IPC/B was detected in the *cwh43*Δ cells expressing the G57R mutant of *CWH43* than in *cwh43*Δ cells expressing wild-type *CWH43*, indicating that mutation of the N-terminal domain causes the instability of the Cwh43 protein. These results suggest that the C-terminal region of Cwh43p is an essential functional domain and that the N-terminal region, which is homologous to PGAP2, supports the function and/or stability of the C-terminal domain.

Rat PGAP2 seems to be identical to FRAG1 (Lorenzi *et al*., 1996), which was isolated from a rat osteosarcoma cell line as a fusion with fibroblast growth factor receptor 2 that has constitutively elevated tyrosine kinase activity due to a chromosomal rearrangement. Recently, rat PGAP2, which is a Golgi/ER-resident membrane protein and conserved in many eukaryotes, was reported to be involved in lipid remodeling from lyso-PI to PI containing saturated fatty acids (Tashima *et al*., 2006; Maeda *et al*., 2007). PGAP2 does not have any known motifs (Tashima *et al*., 2006; Maeda *et al*., 2007). Therefore, it is possible that, like the N-terminal domain of Cwh43p, PGAP2 interacts with an *O*-acyltransferase and that it supports the stability of the enzyme or increases its catalytic activity.

The gene products of mouse *FRAG1* and *C130090K23* are homologues of the N- and C-terminal domains of Cwh43p, respectively. Recombinant mouse C130090K23 protein can remodel the lipid moiety of GPI anchor in yeast cells to ceramides. When both mouse *FRAG1* and *C130090K23* were coexpressed in yeast cells, the gene products coimmunoprecipitated, suggesting that they physically interact with each other, and the coexpression of mouse *FRAG1* enhanced lipid remodeling by C130090K23. This is consistent with the findings in *cwh43*Δ cells introduced with both *CWH43-N* and *CWH43-C*. Because the amino acid sequence of mouse FRAG1 is 97% identical to that of rat PGAP2, mouse FRAG1 is presumably the functional homologue of rat PGAP2, which is involved in the remodeling of lipid from lyso-PI to diacylglycerol containing saturated fatty acids (Tashima *et al*., 2006; Maeda *et al*., 2007). It is possible that mouse FRAG1 protein not only enhances lipid remodeling to ceramides but also the *O*-acyltransferase activity. Thus, further studies should examine whether mouse FRAG1 and human/rat PGAP2 enhance *O*-acyltransferase activity.

It is noteworthy that the mouse *C130090K23* gene product can remodel lipids to ceramides and that *C130090K23* can rescue CFW sensitivity in *cwh43*Δ cells. Therefore, C130090K23 protein is a functional homologue of Cwh43-C. Although ceramides are found in yeast, fungi, parasite, *Dictyostelium*, and certain plants (e.g., pear) (Fankhauser *et al*., 1993; Haynes *et al*., 1993; Ferguson *et al*., 1999; Oxley and Bacic, 1999; Fontaine *et al*., 2003; Pittet and Conzelmann, 2007), they have not been found in the lipid moieties of mammalian GPI-anchored proteins. Thus, it is possible that in some specific tissues where C130090K23 is produced, FRAG1 and C130090K23 associate with each other and participate in the formation of ceramide-type lipid moieties in GPI-anchored proteins. In contrast, in mammalian cells, alkyl/acyl PI moieties are selectively concentrated during the GPI biosynthesis whereas endogenous PI, which is used for the start of GPI biosynthesis, is generally diacyl species (Houjou *et al*., 2007). Although it is unknown what genes are involved in these events and how reactions occurred, it is also possible that C130090K23 might be involved in the uncharacterized lipid remodeling reaction as described above in mammalian cells.

According to SGD, Cwh43p has a DNase I-like region at its C terminus. Isc1p, Inp51p, Inp52p, Inp53p, and Inp54p also have this DNase I-like region. Isc1p is an inositol phosphosphingolipid phospholipase C (Sawai *et al*., 2000), and Inp51/52/53/54 proteins are involved in inositol 5-phosphatase activity (Stolz *et al*., 1998a,b; Guo *et al*., 1999; Wiradjaja *et al*., 2001). Therefore, this motif may be related to the recognition of inositol phosphate, implying that a DNase I-like region in the C-terminal domain of Cwh43p is important for the recognition of inositol phosphate in the GPI anchor. However, it is still unclear whether the conserved D862 and R882 residues, which are likely to be important for its function but are not in the DNase I-like region, are directly involved in the recognition of inositol phosphate.

In this study, we identified how Cwh43p participates in the lipid remodeling of diacylglycerol to ceramides in GPI-anchored proteins; however, how diacylglycerol is replaced with ceramides and what substrate is used for the replacement remains unclear. Future investigations of Cwh43p-mediated lipid remodeling should clarify the molecular mechanism by which the lipid moiety of GPI anchors is replaced with ceramides and its precise biological function.

ACKNOWLEDGMENTS

We are grateful to Ryo Taguchi and Andreas Conzelmann for helpful discussion. We also thank Katsura Hata for providing the anti-Gas1 peptide polyclonal antibody and Roger Tsien for providing the mRFP plasmid. Finally, we thank Michiyo Okamoto and Hiroto Hirayama for stimulating discussions. M.U. was supported by the Hayashi Memorial Foundation for Female Natural Scientists.

REFERENCES

Abe, H., Shimma, Y., and Jigami, Y. (2003). In vitro oligosaccharide synthesis using intact yeast cells that display glycosyltransferases at the cell surface through cell wall-anchored protein Pir. Glycobiology *13*, 87–95.

Altschul, S. F., Madden, T. L., Schaffer, A. A., Zhang, J., Zhang, Z., Miller, W., and Lipman, D. J. (1997). Gapped BLAST and PSI-BLAST: a new generation of protein database search programs. Nucleic Acids. Res. *25*, 3389–3402.

Bagnat, M., Keranen, S., Shevchenko, A., Shevchenko, A., and Simons, K. (2000). Lipid rafts function in biosynthetic delivery of proteins to the cell surface in yeast. Proc. Natl. Acad. Sci. USA *97*, 3254–3259.

Benachour, A., Sipos, G., Flury, I., Reggiori, F., Canivenc-Gansel, E., Vionnet, C., Conzelmann, A., and Benghezal, M. (1999). Deletion of GPI7, a yeast gene required for addition of a side chain to the glycosylphosphatidylinositol (GPI)

core structure, affects GPI protein transport, remodeling, and cell wall integrity. J. Biol. Chem. *274*, 15251–15261.

Benting, J., Rietveld, A., Ansorge, I., and Simons, K. (1999). Acyl and alkyl chain length of GPI-anchors is critical for raft association in vitro. FEBS Lett. *462*, 47–50.

Bickel, T., Lehle, L., Schwarz, M., Aebi, M., and Jakob, C. A. (2005). Biosynthesis of lipid-linked oligosaccharides in *Saccharomyces cerevisiae*: Alg13p and Alg14p form a complex required for the formation of GlcNAc(2)-PP-dolichol. J. Biol. Chem. *280*, 34500–34506.

Bosson, R., Jaquenoud, M., and Conzelmann, A. (2006). GUP1 of *Saccharomyces cerevisiae* encodes an O-acyltransferase involved in remodeling of the GPI anchor. Mol. Biol. Cell *17*, 2636–2645.

Brewis, I. A., Ferguson, M. A., Mehlert, A., Turner, A. J., and Hooper, N. M. (1995). Structures of the glycosyl-phosphatidylinositol anchors of porcine and human renal membrane dipeptidase. Comprehensive structural studies on the porcine anchor and interspecies comparison of the glycan core structures. J. Biol. Chem. *270*, 22946–22956.

Caro, L. H., Tettelin, H., Vossen, J. H., Ram, A. F., van den Ende, H., and Klis, F. M. (1997). In silicio identification of glycosyl-phosphatidylinositol-anchored plasma-membrane and cell wall proteins of *Saccharomyces cerevisiae*. Yeast *13*, 1477–1489.

Conzelmann, A., Puoti, A., Lester, R. L., and Desponds, C. (1992). Two different types of lipid moieties are present in glycophosphoinositol-anchored membrane proteins of *Saccharomyces cerevisiae*. EMBO J. *11*, 457–466.

Fankhauser, C., Homans, S. W., Thomas-Oates, J. E., McConville, M. J., Desponds, C., Conzelmann, A., and Ferguson, M. A. (1993). Structures of glycosylphosphatidylinositol membrane anchors from *Saccharomyces cerevisiae*. J. Biol. Chem. *268*, 26365–26374.

Ferguson, M. A. (1999). The structure, biosynthesis and functions of glycosylphosphatidylinositol anchors, and the contributions of trypanosome research. J. Cell Sci. *112*, 2799–2809.

Ferguson, M. A., Brimacombe, J. S., Brown, J. R., Crossman, A., Dix, A., Field, R. A., Guther, M. L., Milne, K. G., Sharma, D. K., and Smith, T. K. (1999). The GPI biosynthetic pathway as a therapeutic target for African sleeping sickness. Biochim. Biophys. Acta *1455*, 327–340.

Fontaine, T., Magnin, T., Melhert, A., Lamont, D., Latge, J. P., and Ferguson, M. A. (2003). Structures of the glycosylphosphatidylinositol membrane anchors from Aspergillus fumigatus membrane proteins. Glycobiology *13*, 169–177.

Fujita, M., Umemura, M., Yoko-o, T., and Jigami, Y. (2006a). PER1 is required for GPI-phospholipase A2 activity and involved in lipid remodeling of GPI-anchored proteins. Mol. Biol. Ce11 *17*, 5253–5264.

Fujita, M., Yoko-o, T., and Jigami, Y. (2006b). Inositol deacylation by Bst1p is required for the quality control of glycosylphosphatidylinositol-anchored proteins. Mol. Biol. Cell *17*, 834–850.

Fujita, M., Yoko-o, T., Okamoto, M., and Jigami, Y. (2004). GPI7 involved in glycosylphosphatidylinositol biosynthesis is essential for yeast cell separation. J. Biol. Chem. *279*, 51869–51879.

Gao, X. D., Tachikawa, H., Sato, T., Jigami, Y., and Dean, N. (2005). Alg14 recruits Alg13 to the cytoplasmic face of the endoplasmic reticulum to form a novel bipartite UDP-N-acetylglucosamine transferase required for the second step of N-linked glycosylation. J. Biol. Chem. *280*, 36254–36262.

Guillas, I., Pfefferli, M., and Conzelmann, A. (2000). Analysis of ceramides present in glycosylphosphatidylinositol anchored proteins of *Saccharomyces cerevisiae*. Methods Enzymol. *312*, 506–515.

Guo, S., Stolz, L. E., Lemrow, S. M., and York, J. D. (1999). SAC1-like domains of yeast SAC1, INP52, and INP53 and of human synaptojanin encode polyphosphoinositide phosphatases. J. Biol. Chem. *274*, 12990–12995.

Hamada, K., Terashima, H., Arisawa, M., Yabuki, N., and Kitada, K. (1999). Amino acid residues in the omega-minus region participate in cellular localization of yeast glycosylphosphatidylinositol-attached proteins. J. Bacteriol. *181*, 3886–3889.

Haynes, P. A., Gooley, A. A., Ferguson, M. A., Redmond, J. W., and Williams, K. L. (1993). Post-translational modifications of the *Dictyostelium discoideum* glycoprotein PsA. Glycosylphosphatidylinositol membrane anchor and composition of O-linked oligosaccharides. Eur. J. Biochem. *216*, 729–737.

Hirokawa, T., Boon-Chieng, S., and Mitaku, S. (1998). SOSUI: classification and secondary structure prediction system for membrane proteins. Bioinformatics *14*, 378–379.

Horvath, A., Sutterlin, C., Manning-Krieg, U., Movva, N. R., and Riezman, H. (1994). Ceramide synthesis enhances transport of GPI-anchored proteins to the Golgi apparatus in yeast. EMBO J. *13*, 3687–3695.

Houjou, T., Hayakawa, J., Watanabe, R., Tashima, Y., Maeda, Y., Kinoshita, T., and Taguchi, R. (2007). Changes in molecular species profiles of glycosylphosphatidylinositol anchor precursors in early stages of biosynthesis. J. Lipid. Res. *48*, 1599–1606.

Kapteyn, J. C., Van Den Ende, H., and Klis, F. M. (1999). The contribution of cell wall proteins to the organization of the yeast cell wall. Biochim. Biophys. Acta *1426*, 373–383.

Kinoshita, T., and Inoue, N. (2000). Dissecting and manipulating the pathway for glycosylphos-phatidylinositol-anchor biosynthesis. Curr. Opin. Chem. Biol. *4*, 632–638.

Lorenzi, M. V., Horii, Y., Yamanaka, R., Sakaguchi, K., and Miki, T. (1996). FRAG1, a gene that potently activates fibroblast growth factor receptor by C-terminal fusion through chromosomal rearrangement. Proc. Natl. Acad. Sci. USA *93*, 8956–8961.

Maeda, Y., Tashima, Y., Houjou, T., Fujita, M., Yoko-o, T., Jigami, Y., Taguchi, R., and Kinoshita, T. (2007). Fatty acid remodeling of GPI-anchored proteins is required for their raft association. Mol. Biol. Cell *18*, 1497–1506.

Martin-Yken, H., Dagkessamanskaia, A., De Groot, P., Ram, A., Klis, F., and Francois, J. (2001). *Saccharomyces cerevisiae* YCRO17c/CWH43 encodes a putative sensor/transporter protein upstream of the BCK2 branch of the PKC1-dependent cell wall integrity pathway. Yeast *18*, 827–840.

Mayor, S., and Riezman, H. (2004). Sorting GPI-anchored proteins. Nat. Rev. Mol. Cell Biol. *5*, 110–120.

McConville, M. J., Collidge, T. A., Ferguson, M. A., and Schneider, P. (1993). The glycoinositol phospholipids of Leishmania mexicana promastigotes. Evidence for the presence of three distinct pathways of glycolipid biosynthesis. J. Biol. Chem. *268*, 15595–15604.

Okamoto, M., Yoko-o, T., Umemura, M., Nakayama, K., and Jigami, Y. (2006). Glycosylphosphatidylinositol-anchored proteins are required for the transport of detergent-resistant microdomain-associated membrane proteins Tat2p and Fur4p. J. Biol. Chem. *281*, 4013–4023.

Orlean, P., and Menon, A. K. (2007). GPI anchoring of protein in yeast and mammalian cells or: how we learned to stop worrying and love glycophospholipids. J. Lipid. Res. *48*, 993–1011.

Oxley, D., and Bacic, A. (1999). Structure of the glycosylphosphatidylinositol anchor of an arabinogalactan protein from Pyrus communis suspension-cultured cells. Proc. Natl. Acad. Sci. USA *96*, 14246–14251.

Pittet, M., and Conzelmann, A. (2007). Biosynthesis and function of GPI proteins in the yeast *Saccharomyces cerevisiae*. Biochim. Biophys. Acta *1771*, 405–420.

Rayner, J. C., and Munro, S. (1998). Identification of the MNN2 and MNN5 mannosyltransferases required for forming and extending the mannose branches of the outer chain mannans of *Saccharomyces cerevisiae*. J. Biol. Chem. *273*, 26836–26843.

Reggiori, F., Canivenc-Gansel, E., and Conzelmann, A. (1997). Lipid remodeling leads to the introduction and exchange of defined ceramides on GPI proteins in the ER and Golgi of *Saccharomyces cerevisiae*. EMBO J. *16*, 3506–3518.

Sawai, H., Okamoto, Y., Luberto, C., Mao, C., Bielawska, A., Domae, N., and Hannun, Y. A. (2000). Identification of ISC1 (YER019w) as inositol phosphosphingolipid phospholipase C in *Saccharomyces cerevisiae*. J. Biol. Chem. *275*, 39793–39798.

Sherman, F. (1991). Getting started with yeast. Methods Enzymol. *194*, 3–21.

Sikorski, R. S., and Hieter, P. (1989). A system of shuttle vectors and yeast host strains designed for efficient manipulation of DNA in *Saccharomyces cerevisiae*. Genetics *122*, 19–27.

Simons, K., and Ikonen, E. (1997). Functional rafts in cell membranes. Nature *387*, 569–572.

Sipos, G., Puoti, A., and Conzelmann, A. (1994). Glycosylphosphatidylinositol membrane anchors in *Saccharomyces cerevisiae*: absence of ceramides from complete precursor glycolipids. EMBO J. *13*, 2789–2796.

Sipos, G., Reggiori, F., Vionnet, C., and Conzelmann, A. (1997). Alternative lipid remodelling pathways for glycosylphosphatidylinositol membrane anchors in *Saccharomyces cerevisiae*. EMBO J. *16*, 3494–3505.

Stolz, L. E., Huynh, C. V., Thorner, J., and York, J. D. (1998a). Identification and characterization of an essential family of inositol polyphosphate 5-phosphatases (INP51, INP52 and INP53 gene products) in the yeast *Saccharomyces cerevisiae*. Genetics *148*, 1715–1729.

Stolz, L. E., Kuo, W. J., Longchamps, J., Sekhon, M. K., and York, J. D. (1998b). INP51, a yeast inositol polyphosphate 5-phosphatase required for phosphatidylinositol 4,5-bisphosphate homeostasis and whose absence confers a cold-resistant phenotype. J. Biol. Chem. *273*, 11852–11861.

Tanaka, S., Maeda, Y., Tashima, Y., and Kinoshita, T. (2004). Inositol deacylation of glycosylphosphatidylinositol-anchored proteins is mediated by mammalian PGAP1 and yeast Bst1p. J. Biol. Chem. *279*, 14256–14263.

Tashima, Y., Taguchi, R., Murata, C., Ashida, H., Kinoshita, T., and Maeda, Y. (2006). PGAP2 is essential for correct processing and stable expression of GPI-anchored proteins. Mol. Biol. Cell *17*, 1410–1420.

Umemura, M., Okamoto, M., Nakayama, K., Sagane, K., Tsukahara, K., Hata, K., and Jigami, Y. (2003). GWT1 gene is required for inositol acylation of glycosylphosphatidylinositol anchors in yeast. J. Biol. Chem. *278*, 23639–23647.

Wiradjaja, F., Ooms, L. M., Whisstock, J. C., McColl, B., Helfenbaum, L., Sambrook, J. F., Gething, M. J., and Mitchell, C. A. (2001). The yeast inositol polyphosphate 5-phosphatase Inp54p localizes to the endoplasmic reticulum via a C-terminal hydrophobic anchoring tail: regulation of secretion from the endoplasmic reticulum. J. Biol. Chem. *276*, 7643–7653.

Zhu, Y., Vionnet, C., and Conzelmann, A. (2006). Ethanolaminephosphate side chain added to glycosylphosphatidylinositol (GPI) anchor by mcd4p is required for ceramide remodeling and forward transport of GPI proteins from endoplasmic reticulum to Golgi. J. Biol. Chem. *281*, 19830–19839.